Available online at www.sciencedirect.com
ScienceDirect
Icarus 195 (2008) 16–27
ICARUS
www.elsevier.com/locate/icarus

Solar and planetary destabilization of the Earth–Moon triangular Lagrangian points

Jack J. Lissauer [a,*], John E. Chambers [b]

[a] *Space Science and Astrobiology Division, NASA Ames Research Center, Moffett Field, CA 94035, USA*
[b] *Department of Terrestrial Magnetism, Carnegie Institution of Washington, 5241 Broad Branch Rd., NW, Washington, DC 20015, USA*

Received 25 January 2007; revised 30 November 2007

Available online 2 February 2008

Abstract

In the restricted circular three-body problem, two massive bodies travel on circular orbits about their mutual center of mass and gravitationally perturb the motion of a massless particle. The triangular Lagrange points, L_4 and L_5, form equilateral triangles with the two massive bodies and lie in their orbital plane. Provided the primary is at least 27 times as massive as the secondary, orbits near L_4 and L_5 can remain close to these locations indefinitely. More than 2200 cataloged asteroids librate about the L_4 and L_5 points of the Sun–Jupiter system, and five bodies have been discovered around the L_4 point of the Sun–Neptune system. Small satellites have also been found librating about the L_4 and L_5 points of two of Saturn's moons. However, no objects have been discovered around the Earth–Moon L_4 and L_5 points. Using numerical integrations, we show that orbits near the Earth–Moon L_4 and L_5 points can survive for over a billion years even when solar perturbations are included, but the further addition of the far smaller perturbations from other planets destabilize these orbits within several million years. Thus, the lack of observed objects in these regions cannot be used as a constraint on Solar System formation, nor on the tidal evolution of the Moon's orbit.

Keywords: Trojan asteroids; Near-Earth objects; Moon; Earth; Satellites, dynamics

1. Introduction

The general problem of the motion of three or more mutually gravitating bodies is not solvable analytically. However, Lagrange (1772) proved that there are five stationary positions in the restricted circular three-body problem. At these stationary points, a massless (test) particle can remain fixed in a frame rotating with the angular velocity of the two massive bodies. Three of these so-called Lagrangian points lie along the line connecting the two massive bodies; all three of these colinear Lagrangian points are saddle points in the potential, and thus they are unstable in the sense that a particle displaced slightly from any one of them tends to drift away from the equilibrium point. The two other stable points also lie in the plane of the orbit of the massive bodies, and they are the same distance from each of the massive bodies as the massive bodies are from one another; thus, each of these Lagrangian points forms an equilateral triangle with the two massive bodies. The triangular Lagrangian points are potential energy maxima, but they are stabilized by Coriolis forces provided the primary is $> (29 + \sqrt{621})/2 \approx 26.96$ times as massive as the secondary. [See Danby (1988) for a derivation and further details.] The triangular Lagrangian point leading (trailing) the secondary body in orbit is denoted L_4 (L_5).

More than two thousand asteroids are currently known to orbit near and librate about the L_4 and L_5 triangular Lagrangian points of the Sun–Jupiter system (http://ssd.jpl.nasa.gov/et_form.html); these asteroids are known as the trojans. Numerical models show that test particles in regions near the triangular Lagrangian points of the other giant planets can also survive for the age of the Solar System, although the immediate vicinity of Saturn's L_4 and L_5 points are unstable, and in general planetary perturbations make the regions near the L_4 and L_5 points of Saturn and Uranus less stable than those near the L_4 and L_5 points of Jupiter and Neptune (Innanen and Mikkola, 1989; Nesvorný and Dones, 2002). No L_4 and L_5 librators of Sat-

* Corresponding author.
E-mail address: jack.j.lissauer@nasa.gov (J.J. Lissauer).

0019-1035/$ – see front matter
doi:10.1016/j.icarus.2007.12.024

Table 1
Initial coordinates of test particles (simulations with all planets)

Region	δa (10^{-5} AU)[a]	$\delta\lambda$ (°)[a]	e[a]	ϖ (°)[a]	i (°)[b]	Ω (°)[a]	Number of particles	Figure #
L_4	−5, 5, 1	55, 67, 1	0.02, 0.2, 0.02	0, 330, 30	0	–	17,160	1a
L_4	−3.5, 0.5, 0.4	61, 67, 0.5	0.07, 0.15, 0.01	310, 350, 5	0	–	11,583	1b
L_4	$-2.2, -0.2, 0.3\overline{3}$	63.25, 65.25, 0.5	0.11, 0.125, 0.005	322, 334, 4	0	–	560	1c
L_4	−2, −0.5, 0.3	63.5, 64.7, 0.3	0.113, 0.122, 0.003	325, 331, 2	0	–	480	1d
L_5	−5, 5, 1	−67, −55, 1	0.02, 0.2, 0.02	0, 330, 30	0	–	17,160	2a
L_5	−2, 2, 0.4	−64, −58, 0.5	0.09, 0.17, 0.01	250, 290, 5	0	–	11,583	2b
L_5	−1.6, 0.8, 0.4	−62, −60, 0.5	0.125, 0,155, 0.01	264, 276, 4	0	–	700	2c
L_4	−5, 5, 2	55, 67, 3	0.04, 0.2, 0.04	0, 270, 90	0.5, 1, 2, 4, 8	0, 270, 90	12,000	3a
L_4	−2, 2, 1	60, 66, 1.5	0.08, 0.16, 0.02	160, 200, 10	0.5, 1, 2, 4, 8	0, 270, 90	12,500	3b
L_4	−2, −0.5, 0.3	63.5, 64.7, 0.3	0.113, 0.122, 0.003	325, 331, 2	0.5, 1, 2, 4, 8	0, 270, 90	9600	3c
L_5	−5, 5, 2	−67, −55, 3	0.04, 0.2, 0.04	0, 270, 90	0.5, 1, 2, 4, 8	0, 270, 90	12,000	4a
L_5	−1, 3, 1	−64, −58, 1.5	0.1, 0.18, 0.02	250, 290, 10	0.5, 1, 2, 4, 8	0, 270, 90	10,000	4b
L_5	−1.4, 0.1, 0.3	−61.6, −60.4, 0.3	0.118, 0.136, 0.006	267, 273, 2	1, 2	0, 270, 90	3840	4c
L_4	−5, 5, 2.5	54, 66, 3	0.02, 0.1, 0.02	0, 288, 72	30, 35, 40, 45, 50	0, 324, 36	31,250	5

[a] The numbers listed represent the minimum value, maximum value, and spacing between values of the specified parameter.
[b] Listing of values of inclination used.

urn and Uranus have yet been found, but five Neptune L_4 point librators have been identified (Sheppard and Trujillo, 2006; http://cfa-www.harvard.edu/iau/lists/NeptuneTrojans.html).

The Earth/Moon mass ratio of 81.3 is suitable for L_4 and L_5 point stability, and simulations of lunar formation find that some debris often remain trapped in horseshoe orbits encompassing three trojan points (Kokubo et al., 2000). However, despite numerous searches (Valdes and Freitas, 1983 and references therein), no objects have been detected librating about the triangular Lagrangian points of the Earth–Moon system. High-precision numerical integrations that include the Sun, Moon and planets demonstrate that some test particles initially near the Earth–Moon L_4 and L_5 points remain there for at least the 1000 years that these studies have simulated (Jorba, 2000); included among the survivors is a group with high inclination. Earth–Moon trojans may have been destabilized billions of years ago when tidal recession of the Moon caused the system to pass through a resonance with the Sun (Ćuk et al., 2006). We study herein the fates of such particles on million year time scales at the current epoch.

2. Numerical experiments

We performed numerical integrations of test particles initially located near the Earth–Moon L_4 point for the Earth–Moon–Sun case and for particles near both the L_4 and L_5 points including all eight planets together with the Moon and the Sun. When complicating factors such as orbital eccentricity and additional perturbers are present, the triangular points are not necessarily the locations of the most stable orbits for test particles (Nesvorný and Dones, 2002). Thus, we conducted our numerical investigations on a grid of initial particle phase space locations centered upon each triangular Lagrangian point of the Earth–Moon system. The phase space of possible initial test particle state vectors has six dimensions, representing the position and velocity of the particle or an equivalent set of orbital elements. We chose to select initial conditions on a grid of the following geocentric orbital elements: δa, representing the difference between the particle's semimajor axis and that of the Moon; $\delta\lambda$, the difference between the particle's mean longitude and that of the Moon; e, eccentricity; $\delta\varpi$, the difference between the particle's longitude of perigee and that of the Moon; i, inclination of the particle's orbit relative to that of the Moon; Ω, the longitude of the particle's ascending node relative to the Earth–Moon line of nodes. All integrations apart from the Earth–Moon–Sun high eccentricity case were begun at the epoch 2002 Jan 01 0:0 hours = JD 2452275.5. The masses and initial coordinates and velocities for all massive bodies were taken from JPL's horizon telnet site.

Particles were removed when they collided with the Moon or the Earth, or when they reached a distance of 1 AU from the Earth. In the early stages of our numerical simulations, the most common end state is collision with the Moon. Later, most remaining test particles escape from geocentric orbit and drift 1 AU away. Only a small fraction actually hit Earth (prior to escaping from the Earth–Moon system). Every particle in the integrations that included all of the planets was followed until it either hit the Earth or the Moon or escaped from the Earth–Moon system. The Earth–Moon–Sun integrations with current

Fig. 1. Lifetimes of test particles near the L_4 leading Lagrangian point of the Earth–Moon system are displayed as a function of initial particle position. The plots represent the results of a four-dimensional survey in initial δa (difference between the semimajor axis of the particle and that of the Moon), $\delta\lambda$ (mean longitude with respect to the Moon), e (eccentricity), ϖ (longitude of periapse) phase space. For each value of a and λ, the circles represent results for the initial eccentricities shown by the color bar at the right. The diameter of the circle is proportional to the logarithm of the lifetime (in years) of the longest-surviving particle with initial coordinates given (among the several particles with differing ϖ that were simulated) in our integrations that included the Moon, the Sun and all eight planets. The small and large concentric circles below the color bar represent lifetimes of 1000 and 10^6 years, respectively. Panel (a) shows results from our coarsest grid that contained 17,160 particles, and the following panels show progressively finer grids in the region (denoted by dashed line boxes) of the longest-lived particles. Note that although the longest-lived particles are concentrated in a particular region in panels (a) and (b), no well-defined peak is present in the panel (d). Black crosses mark the initial locations of particles that were stable for 1 Gyr in the Earth–Moon–Sun simulations.

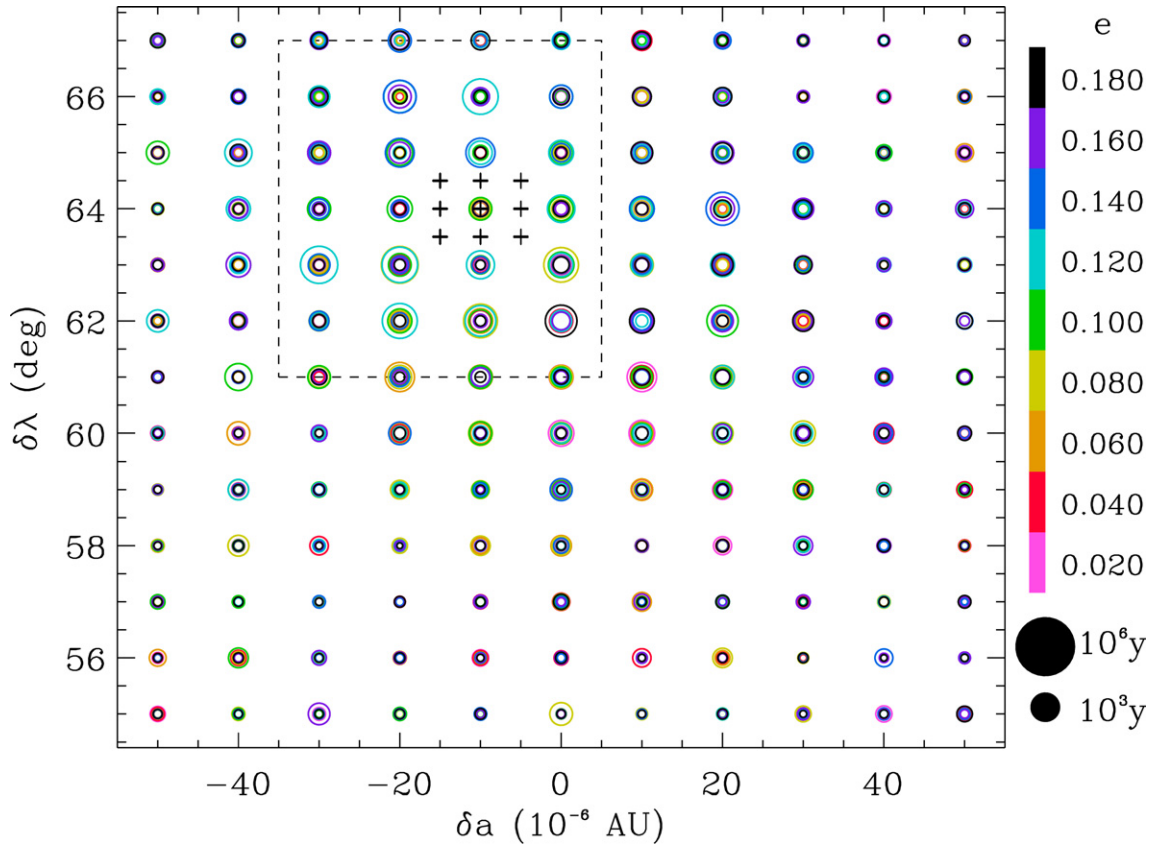
e
0.180
0.160
0.140
0.120
0.100
0.080
0.060
0.040
0.020
10⁶y
10³y
δλ (deg)
66
64
62
60
58
56
−40
−20
0
20
40
δa (10⁻⁶ AU)

(a)

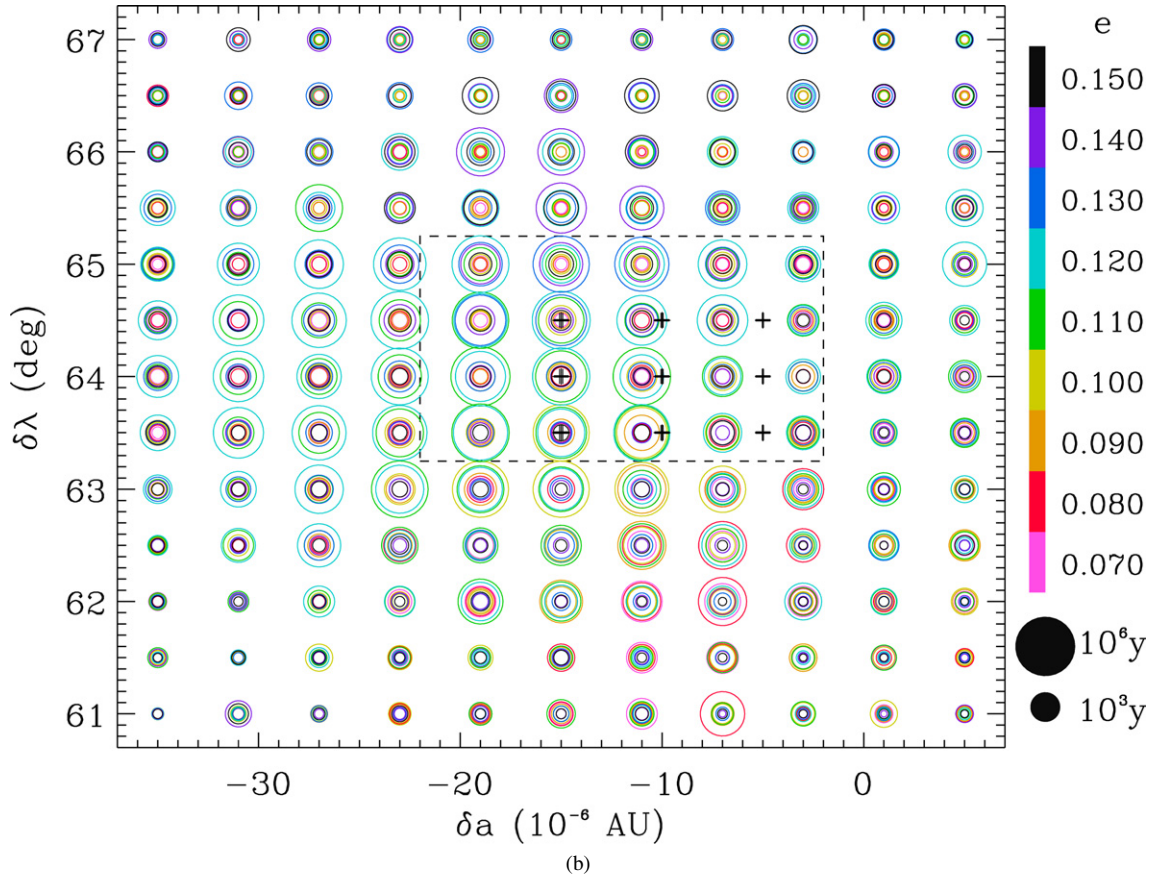
e
0.150
0.140
0.130
0.120
0.110
0.100
0.090
0.080
0.070
10⁶y
10³y
δλ (deg)
67
66
65
64
63
62
61
−30
−20
−10
0
δa (10⁻⁶ AU)

(b)

Fig. 1.

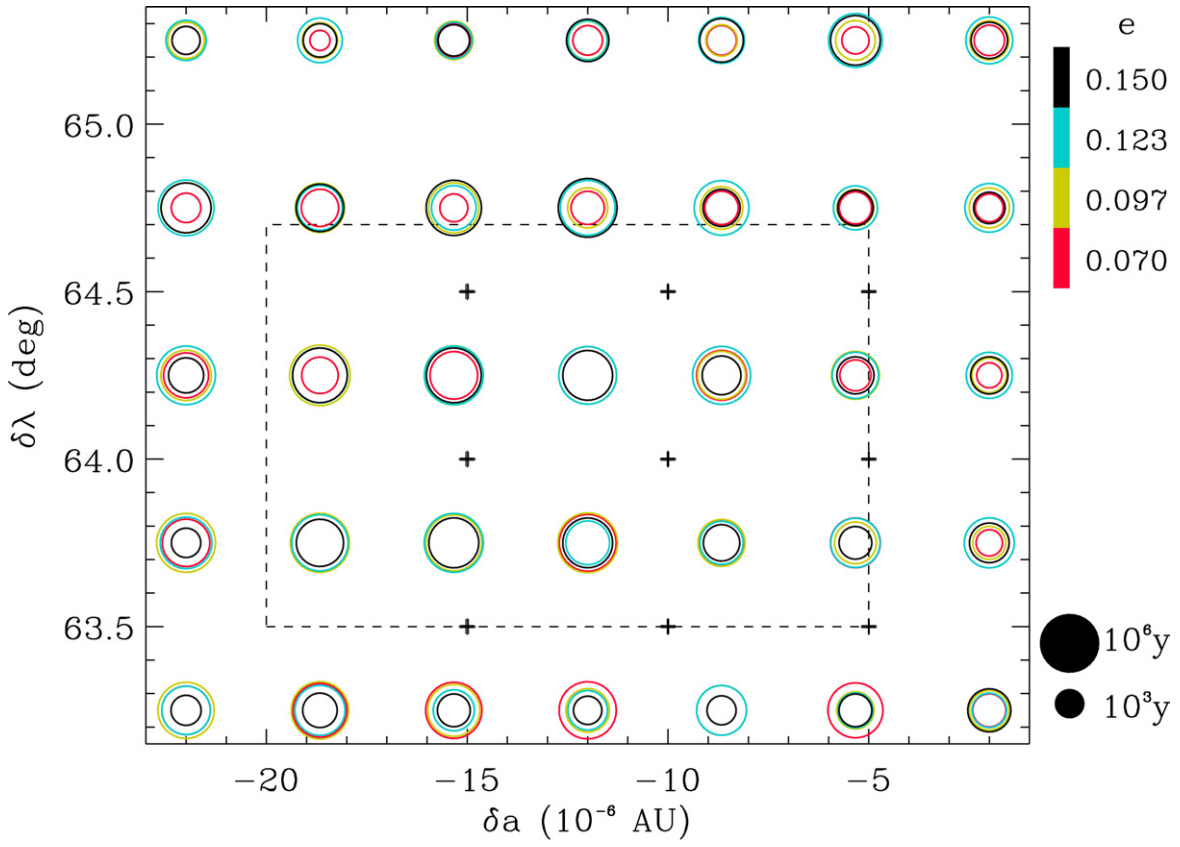

(c)

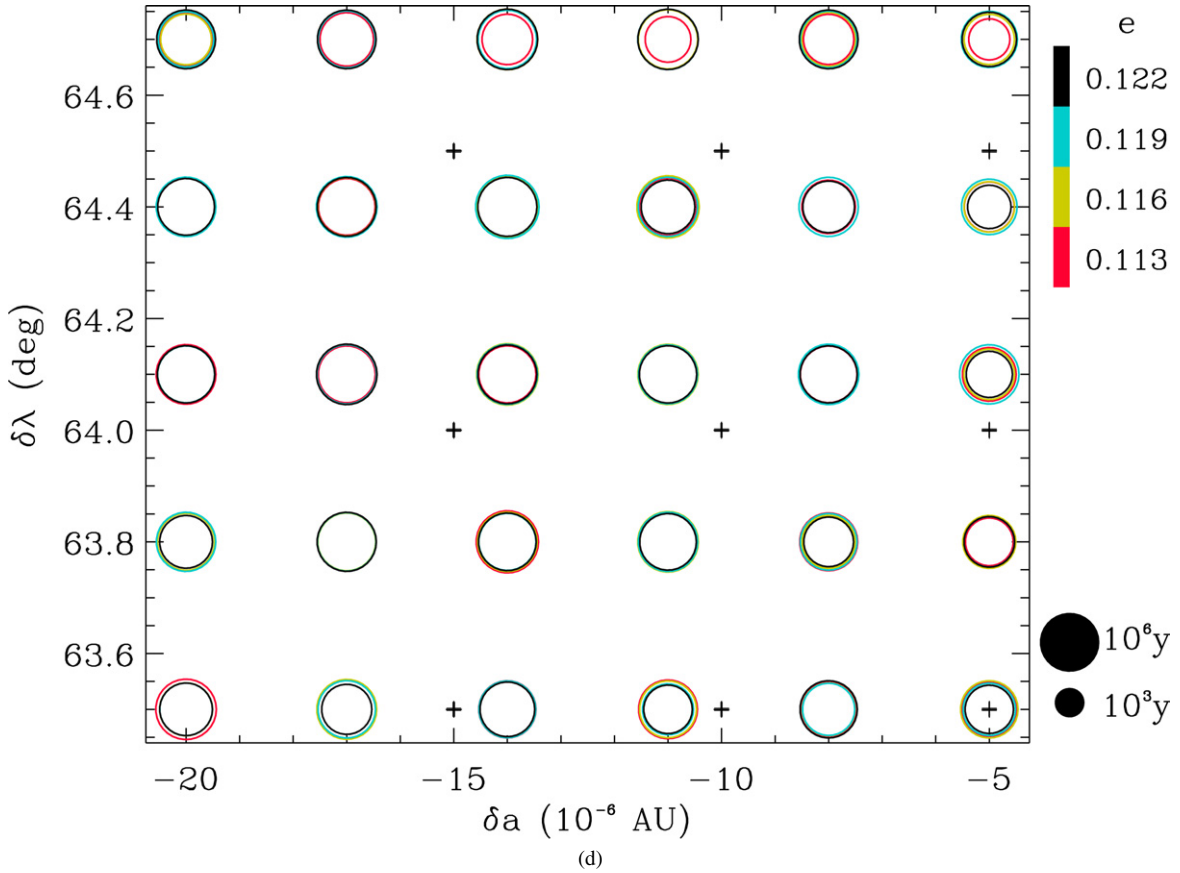

(d)

Fig. 1. (*continued*)

eccentricity were terminated after 1 billion years and those with high eccentricity were terminated after 100 million years.

Our 8 planet integrations used Everhart's RADAU integrator algorithm (Everhart, 1985) as implemented in the Mercury integration package (Chambers, 1999). This is a moderately efficient, highly accurate, high-order integrator. We began by integrating on coarse grids centered at each of the two triangular Lagrangian points. We conducted four-dimensional surveys of test particles initially orbiting in the same plane as the Moon with initial semimajor axes from -5×10^{-5} AU $\leqslant \delta a \leqslant 5 \times 10^{-5}$ AU in steps of 1×10^{-5} AU, initial longitudes from $55° \leqslant |\delta\lambda| \leqslant 67°$ in steps of 1°, initial eccentricity $0.02 \leqslant e \leqslant 0.18$ in steps of 0.02 and initial perigee angles, ϖ, spread uniformly in longitude at intervals of 30°. The initial grids for our survey of moderately inclined particles were δa: -5×10^{-5} to $+5 \times 10^{-5}$ in steps of 2×10^{-5}; $|\delta\lambda|$: 55 to 67° in steps of 3°; e: 0.04 to 0.20 in steps of 0.04; $\delta\varpi$: 0 to 270° in steps of 90°; $i = 0.5, 1, 2, 4, 8°$; Ω: 0 to 270° in steps of 90°. Thus, we began with 17,160 particles on in-plane orbits and 12,000 particles on moderately inclined orbits around each of the triangular Lagrangian points. We subsequently zoomed-in to conduct higher resolution investigations of the regions in which particles survived for the longest times and integrated particles on finer grids within these regions. We also followed 31,250 highly inclined ($30° \leqslant i \leqslant 50°$) particles near L_4. The initial parameter ranges and spacings for all of our 8 planet runs are given in Table 1.

The lifetimes of the longest-lived particles in our planar 8 planet integrations around L_4 are displayed graphically in Fig. 1. Figs. 2–5 present analogous plots for planar integrations in the vicinity of L_5, moderately inclined orbits about L_4, moderately inclined orbits about L_5, and highly inclined orbits about L_4, respectively. No particle in our planar or moderately inclined orbit integrations that included all of the planets survived for even 3 million years. In the initial and second simulations around each Lagrangian point, there are regions in phase space where particle lifetimes are longest, so we zoomed in on these regions and examined progressively higher resolution grids in phase space. However, in the final simulations around each Lagrangian point, no unresolved region of $\delta a - \delta\lambda$ phase space appears to be preferred (Figs. 1d, 2c, 3c and 4c). The longest-lived particle in our highly inclined simulations, which began with $\delta a = -5 \times 10^{-5}$ to $+5 \times 10^{-5}$; $|\delta\lambda| = 57°$; $e = 0.04$; $\delta\varpi = 72°$; $i = 35°$; $\Omega = 36°$, survived for 3.48 Myr, the second longest, with $i = 30°$, for 2.74 Myr, and all other

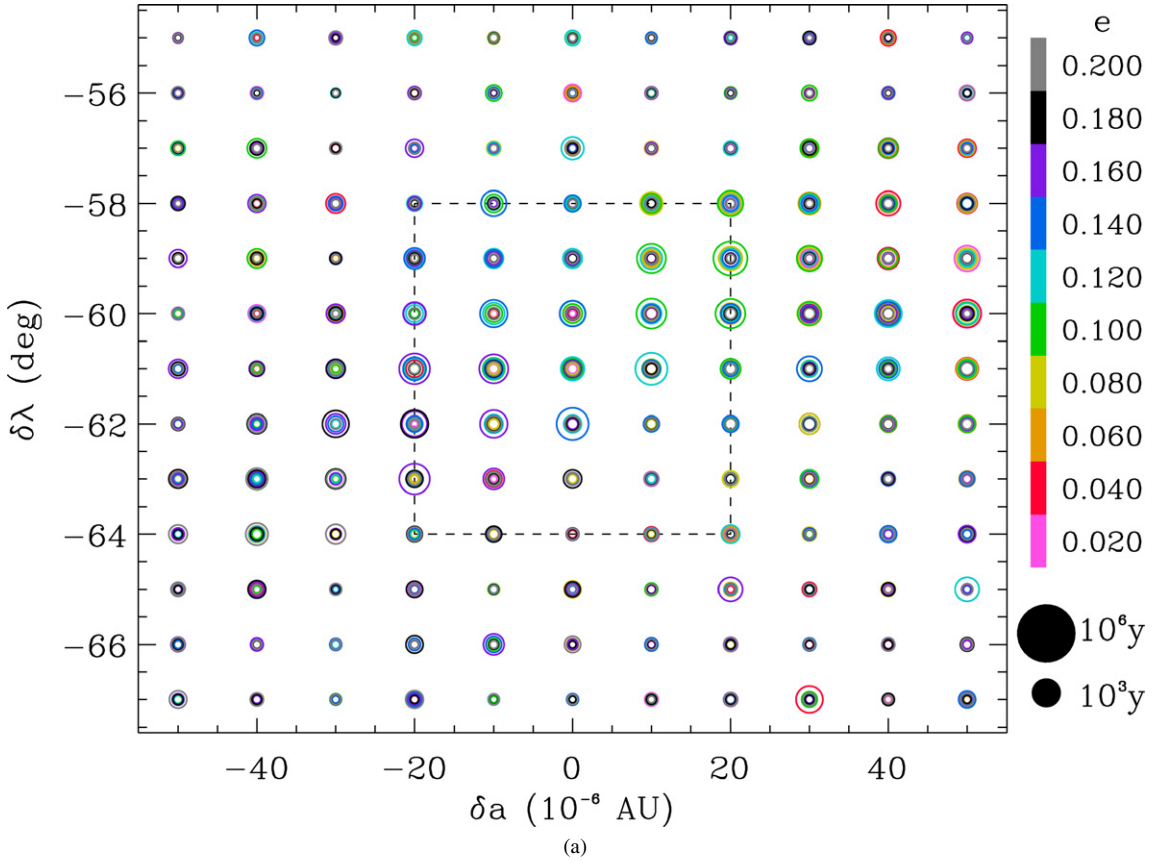

(a)

Fig. 2. Lifetimes of test particles near the L_5 trailing Lagrangian point of the Earth–Moon system are displayed as a function of initial particle position. The plots represent the results of a four-dimensional survey in initial δa (difference between the semimajor axis of the particle and that of the Moon), $\delta\lambda$ (mean longitude with respect to the Moon), e (eccentricity), ϖ (longitude of periapse) phase space. For each value of a and λ, the circles represent results for the initial eccentricities shown by the color bar at the right. The diameter of the circle is proportional to the logarithm of the lifetime (in years) of the longest-surviving particle with initial coordinates given (among the several particles with differing ϖ that were simulated) in our integrations that included the Moon, the Sun and all eight planets. The small and large concentric circles below the color bar represent lifetimes of 1000 and 10^6 years, respectively. Panel (a) shows results from our coarsest grid that contained 17,160 particles, and the following panels show progressively finer grids in the region (denoted by dashed line boxes) of the longest-lived particles.

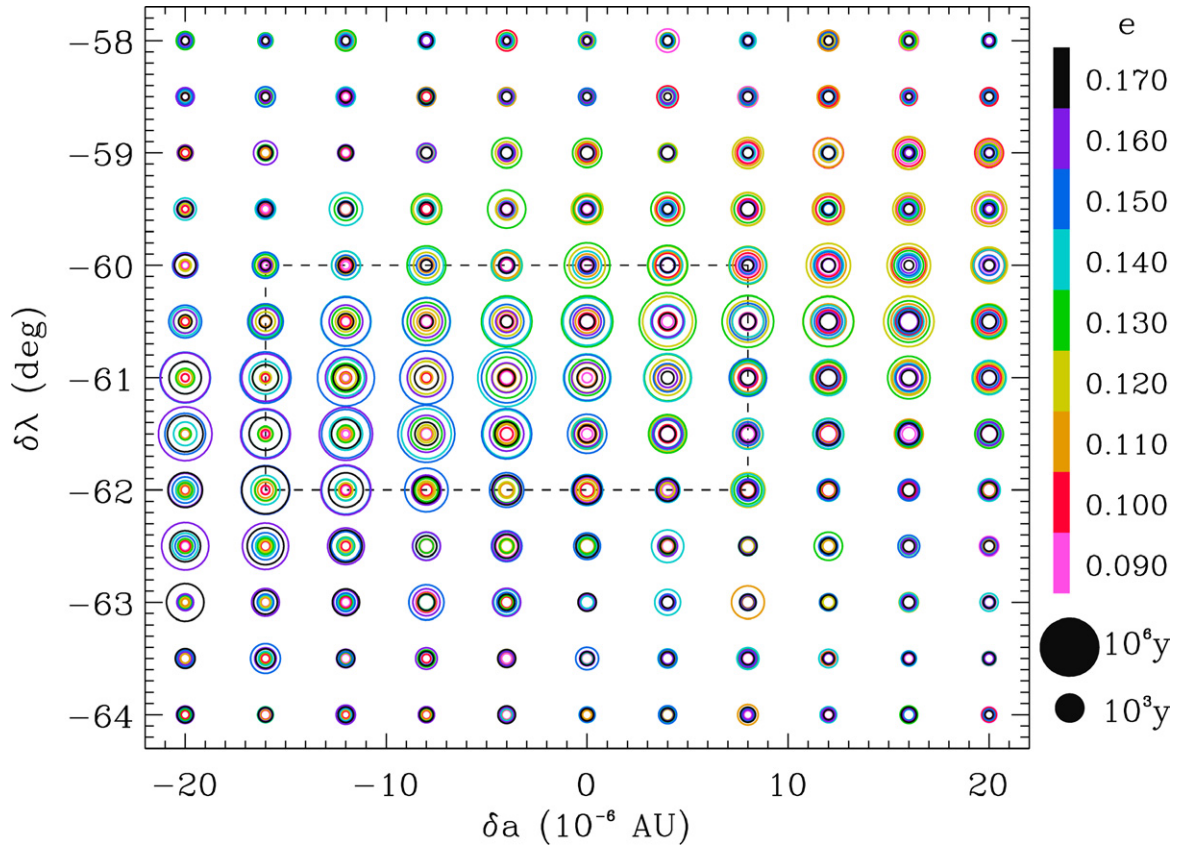

(b)

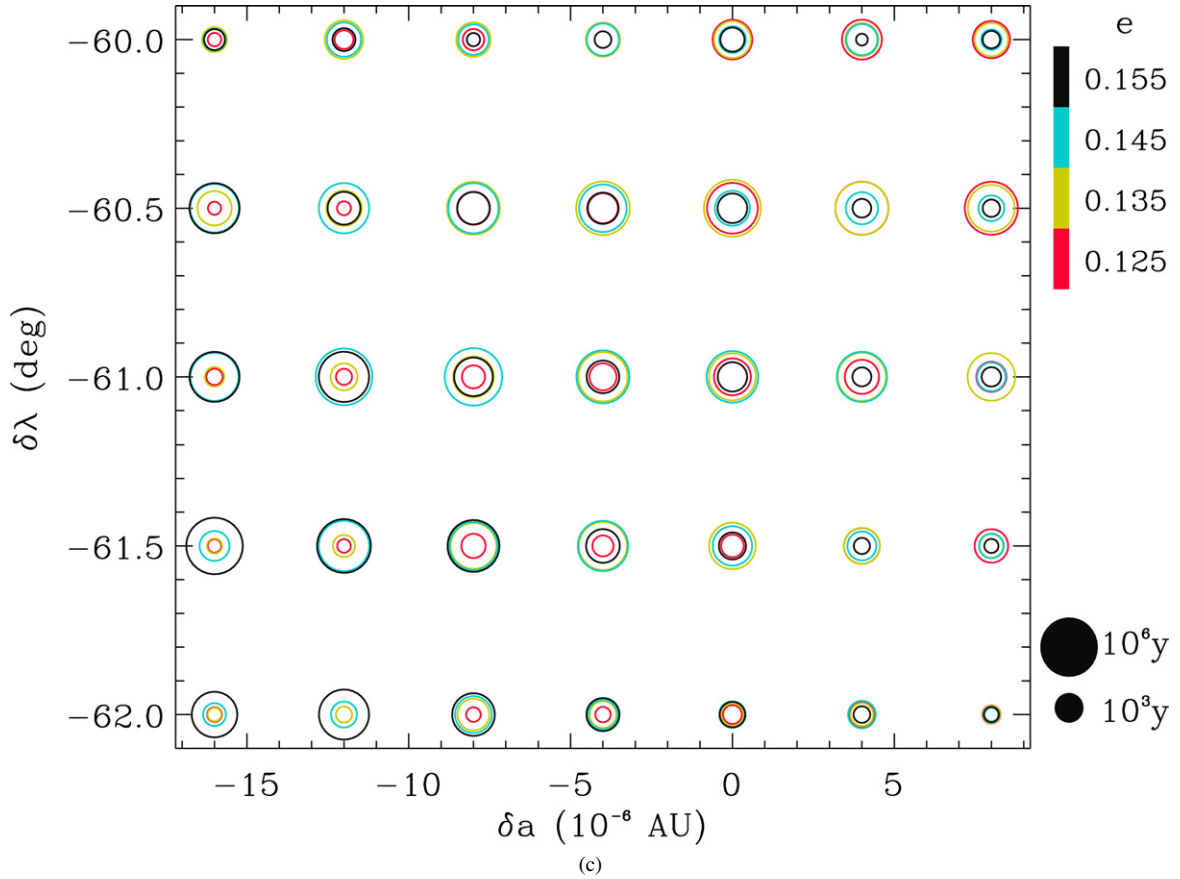

(c)

Fig. 2. (*continued*)

particles were lost in <1.77 Myr. Because there was no region of this part of phase space that seemed to be especially stable, we did not zoom-in around the longest-lived particles in our high i runs. While a higher resolution survey of this chaotic phase space would almost certainly identify somewhat longer-lived orbits, it is quite unlikely that trajectories which remain near either of the Earth–Moon triangular points for a substantial fraction of the age of the Solar System would be found. The particular initial locations of the most stable orbits would differ if we changed the starting epoch by even a small amount, but characteristic lifetimes of these orbits would not.

In order to determine the reason(s) that particles cannot remain in the vicinity of the Earth–Moon triangular Lagrangian points for geological time scales, we performed integrations of test particles in the Earth–Moon–Sun restricted 4-body problem. Our first set of integrations for the Earth–Moon–Sun case used a version of Wisdom and Holman's mixed-variable symplectic mapping modified for wide binary systems (i.e., Earth–Sun) that is described in Chambers et al. (2002). The central body was the Earth. The wide-binary companion was the Sun. The Moon and test particles were assumed to be orbiting the Earth, while receiving perturbations from the Sun (the distant binary companion). We conducted a four-dimensional survey of test particles initially orbiting near L_4 in the same plane as the Moon in a region where particles in the 8 planet integrations were relatively long-lived. We followed 81 particles with initial semimajor axes from -1.5×10^{-5} AU $\leqslant \delta a \leqslant 0.55 \times 10^{-5}$ AU in steps of 0.5×10^{-5} AU, initial longitudes from $63.5° \leqslant |\delta\lambda| \leqslant 64.5°$ in steps of 0.5°, initial eccentricity $0.115 \leqslant e \leqslant 0.125$ in steps of 0.005 and initial perigee angles, ϖ, from −34° to −30° in steps of 2°. In contrast to the 8 planet integrations, when the only forces considered are the Newtonian gravitational attraction of the Earth, Moon and Sun 27 test particles remained in the vicinity of the L_4 triangular Lagrangian point of the Earth–Moon system for the entire one billion years that we simulated (crosses in Figs. 1 and 3). We did not perform analogous restricted 4-body simulations around the L_5 point. The total fractional energy error during 10^9 year integration was 1.5×10^{-8} and the total fractional angular momentum error was 1.5×10^{-11}.

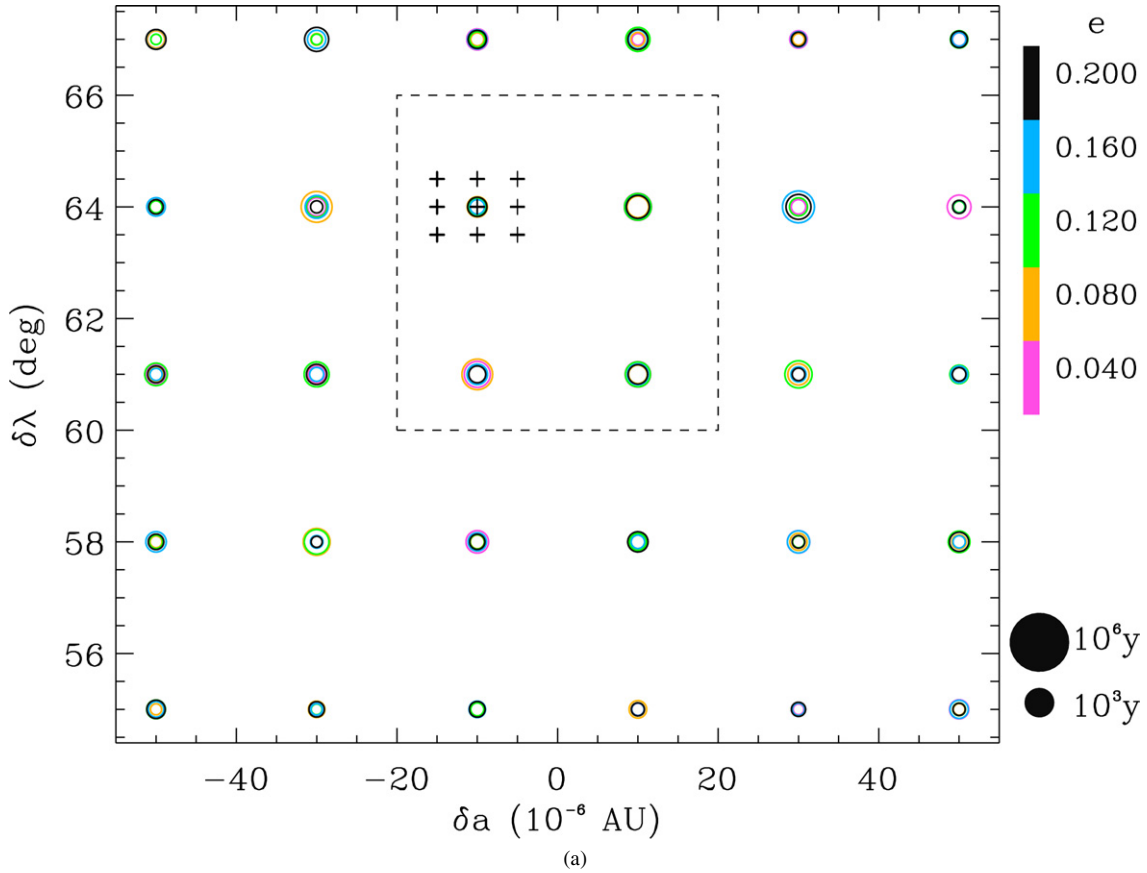

(a)

Fig. 3. Lifetimes of test particles beginning on moderately inclined orbits near the L_4 leading Lagrangian point of the Earth–Moon system are displayed as a function of initial particle position. The plots represent the results of a six-dimensional survey in initial δa (difference between the semimajor axis of the particle and that of the Moon), $\delta\lambda$ (mean longitude with respect to the Moon), e (eccentricity), ϖ (longitude of periapse), i (inclination), Ω (longitude of the particle's ascending node relative to the Earth–Moon line of nodes) phase space. For each value of a and λ, the circles represent results for the initial eccentricities shown by the color bar at the right. The diameter of the circle is proportional to the logarithm of the lifetime (in years) of the longest-surviving particle with initial coordinates given (among the several particles with differing ϖ, i, and Ω that were simulated) in our integrations that included the Moon, the Sun and all eight planets. The small and large concentric circles below the color bar represent lifetimes of 1000 and 10^6 years, respectively. Panel (a) shows results from our coarsest grid that contained 12,000 particles, and the following panels show progressively finer grids in the region (denoted by dashed line boxes) of the longest-lived particles. Black crosses mark the initial locations of particles that were stable for 1 Gyr in the Earth–Moon–Sun simulations.

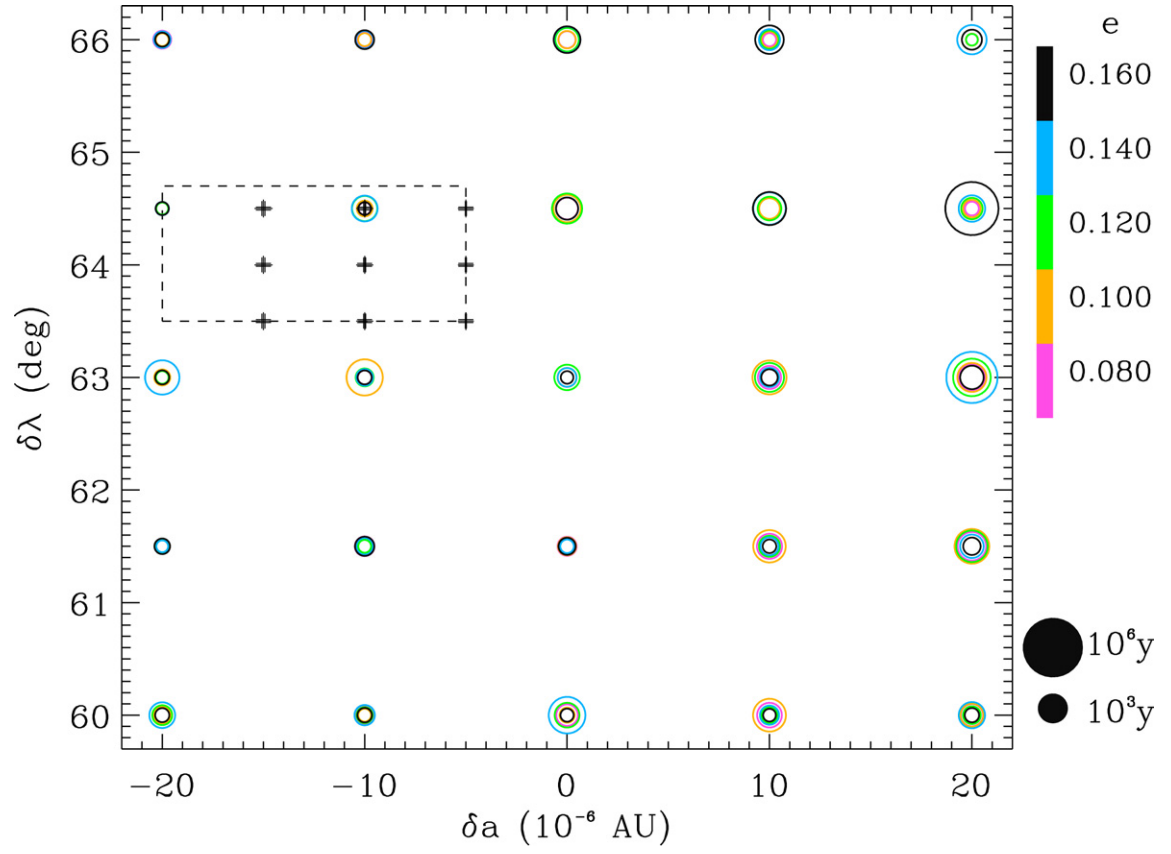

(b)

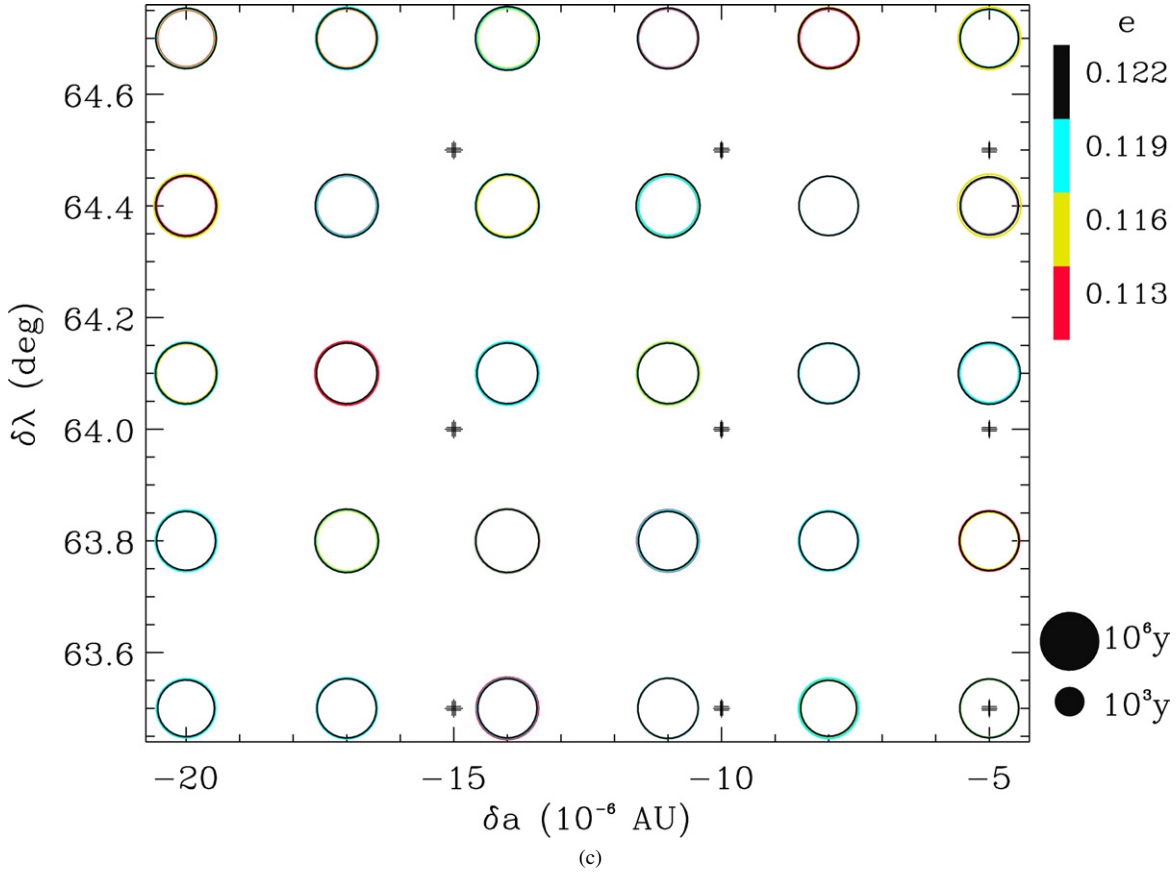

(c)

Fig. 3. (*continued*)

Although planetary perturbations are orders of magnitude smaller than solar perturbations, they change the eccentricity of Earth's orbit about the Sun. Particles are lost more rapidly when Earth's orbital eccentricity is high and increasing, but variations in the value of Earth's heliocentric inclination have relatively little effect (Fig. 6). This suggests that the planets indirectly affect the orbits of particles near the Earth–Moon L_4 and L_5 points through solar perturbations, either because high eccentricity of the Earth's orbit causes problems or because variations in eccentricity of the orbit destabilize the Earth–Moon triangular Lagrangian points. Alternatively, planetary resonances analogous to those that may have excited lunar eccentricity (Ćuk, 2007) may more directly destabilize test particles placed near the Earth–Moon triangular Lagrangian points. In order to distinguish between these three possibilities, we conducted additional restricted 4-body integrations; all of these simulations used the RADAU integrator.

We investigated the effects of increased solar eccentricity by performing a restricted 4-body simulation in which the initial positions and velocities of the Sun and Earth were taken from an integration of the Sun plus 8 planets done using RADAU until a point when the Earth was close to a maximum in its eccentricity. The initial orbital elements of the Sun were: $a = 0.9991711$ AU, $e = 0.0618808$, $i = 0.7350°$, $\varpi = 302.5934°$, $\Omega = 6.2966°$, $\lambda = 162.4466°$, with the key factor being that e was much larger than it is at the present epoch. A total of 1296 particles were integrated about the L_4 point in a $6 \times 6 \times 6 \times 6$ array with initial semimajor axes from 3×10^{-5} AU $\leqslant \delta a \leqslant 4 \times 10^{-5}$ AU in steps of 0.2×10^{-5} AU, initial longitudes from $58.6° \leqslant |\delta\lambda| \leqslant 61.1°$ in steps of 0.3°, initial eccentricity $0.07 \leqslant e \leqslant 0.09$ in steps of 0.004 and initial perigee angles, ϖ, from 263° to 273° in steps of 2°. The initial positions and velocities of the Moon with respect to Earth were same as in the main integrations, so apart from the test particle grid, the only thing that changed was the initial position and velocity of the Sun in the 4-body problem. There were 143 survivors out of 1296 particles after 100 Myr. Thus, larger but constant eccentricity of the Earth's heliocentric orbit, within the range forced by the planets, does not completely destabilize the Earth–Moon triangular Lagrangian points.

Our final pair of numerical experiments compared the evolution in the restricted 4-body problem with that including the same objects but adding an artificial growth in the Sun's eccentricity about the Earth. The initial particles were the same as

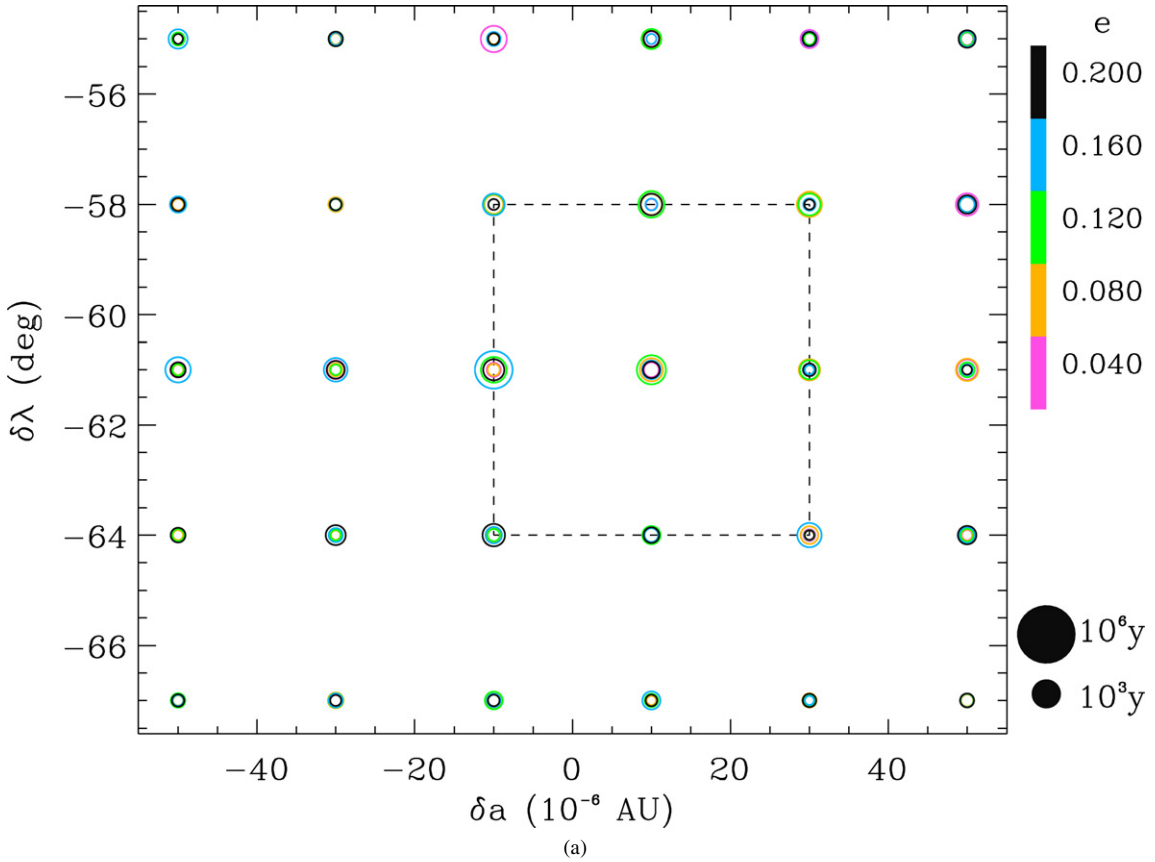

(a)

Fig. 4. Lifetimes of test particles beginning on moderately inclined orbits near the L_5 trailing Lagrangian point of the Earth–Moon system are displayed as a function of initial particle position. The plots represent the results of a six-dimensional survey in initial δa (difference between the semimajor axis of the particle and that of the Moon), $\delta\lambda$ (mean longitude with respect to the Moon), e (eccentricity), ϖ (longitude of periapse), i (inclination), Ω (longitude of the particle's ascending node relative to the Earth–Moon line of nodes) phase space. For each value of a and λ, the circles represent results for the initial eccentricities shown by the color bar at the right. The diameter of the circle is proportional to the logarithm of the lifetime (in years) of the longest-surviving particle with initial coordinates given (among the several particles with differing ϖ, i, and Ω that were simulated) in our integrations that included the Moon, the Sun and all eight planets. The small and large concentric circles below the color bar represent lifetimes of 1000 and 10^6 years, respectively. Panel (a) shows results from our coarsest grid that contained 12,000 particles, and the following panels show progressively finer grids in the region (denoted by dashed line boxes) of the longest-lived particles.

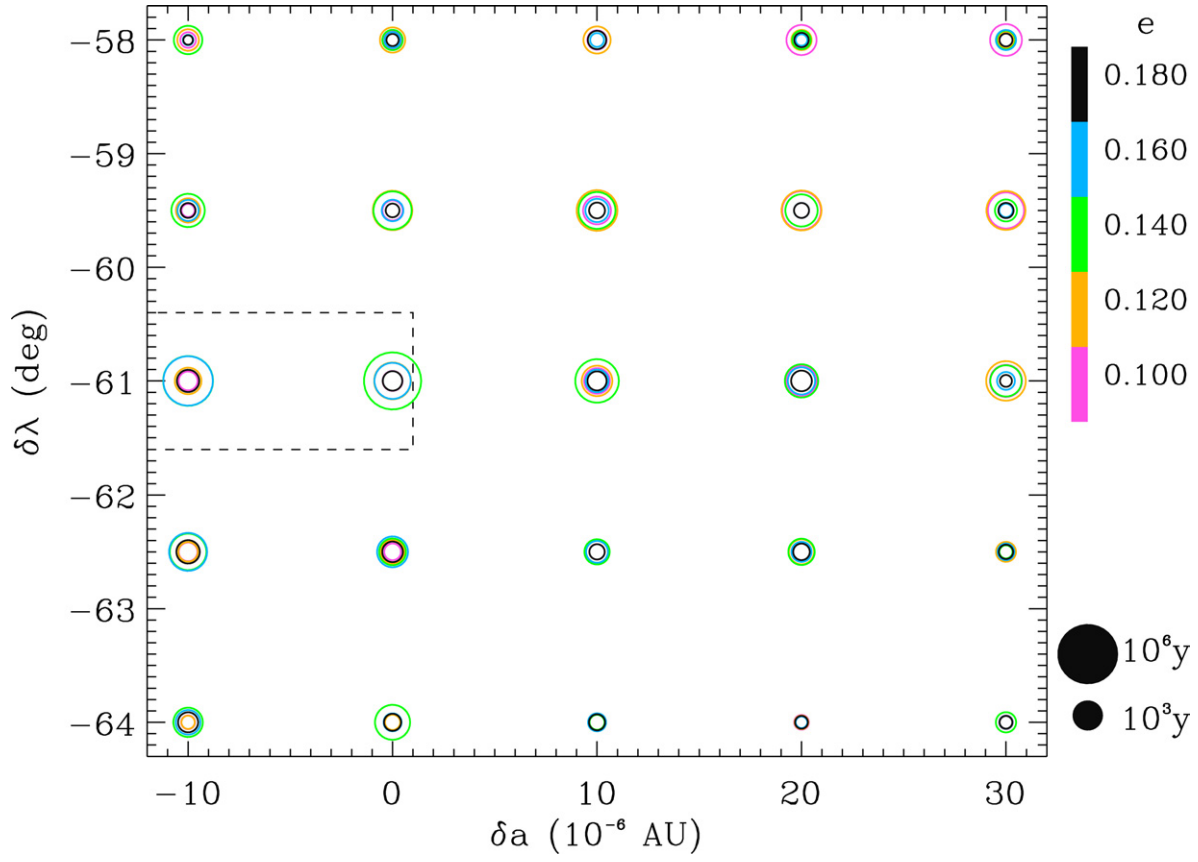

(b)

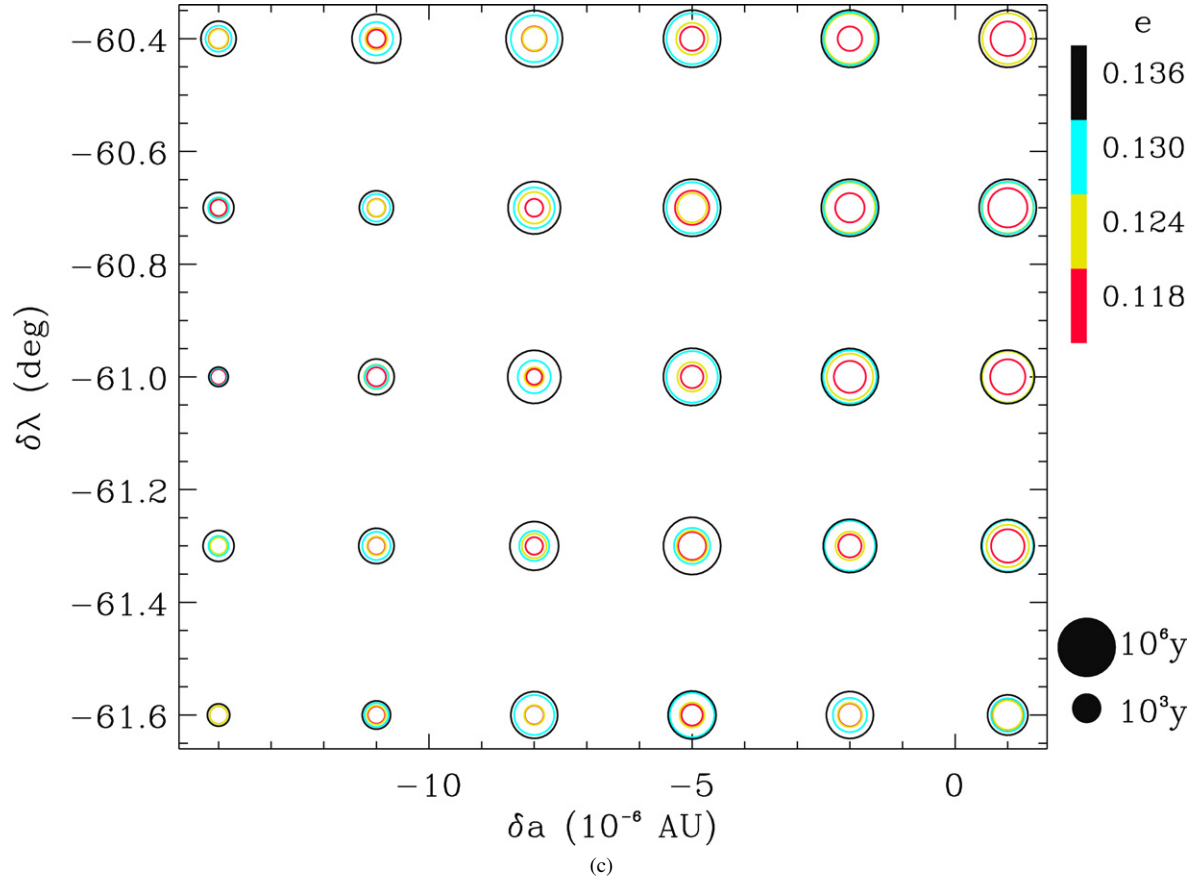

(c)

Fig. 4. (*continued*)

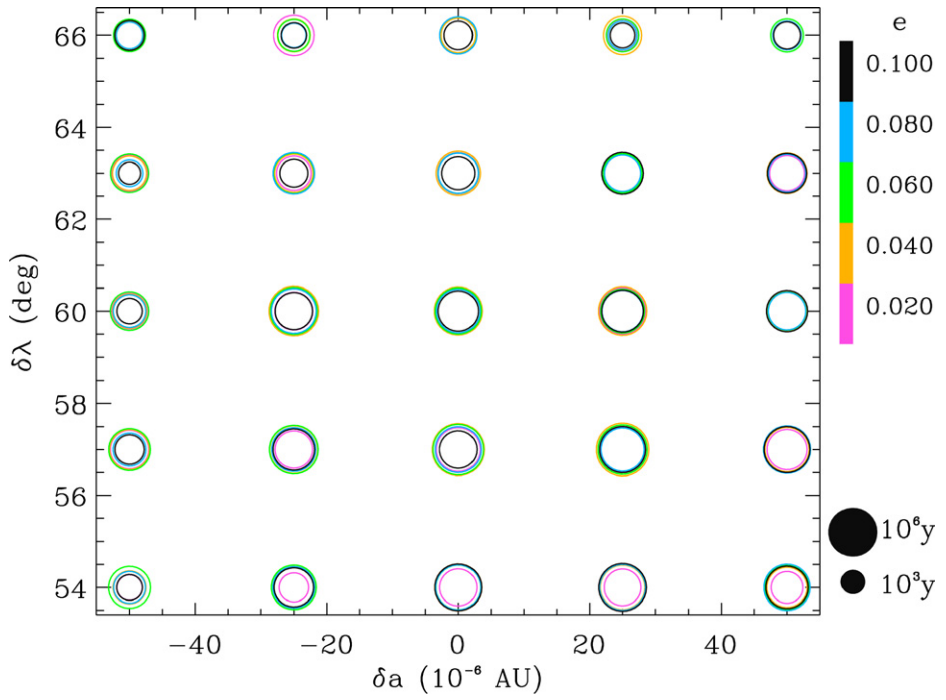

Fig. 5. Lifetimes of test particles beginning on highly inclined orbits near the L_4 leading Lagrangian point of the Earth–Moon system are displayed as a function of initial particle position. The plots represent the results of a six-dimensional survey in initial δa (difference between the semimajor axis of the particle and that of the Moon), $\delta\lambda$ (mean longitude with respect to the Moon), e (eccentricity), ϖ (longitude of periapse), i (inclination), Ω (longitude of the particle's ascending node relative to the Earth–Moon line of nodes) phase space. For each value of a and λ, the circles represent results for the initial eccentricities shown by the color bar at the right. The diameter of the circle is proportional to the logarithm of the lifetime (in years) of the longest-surviving particle with initial coordinates given (among the several particles with differing ϖ, i, and Ω that were simulated) in our integrations that included the Moon, the Sun and all eight planets. The small and large concentric circles below the color bar represent lifetimes of 1000 and 10^6 years, respectively.

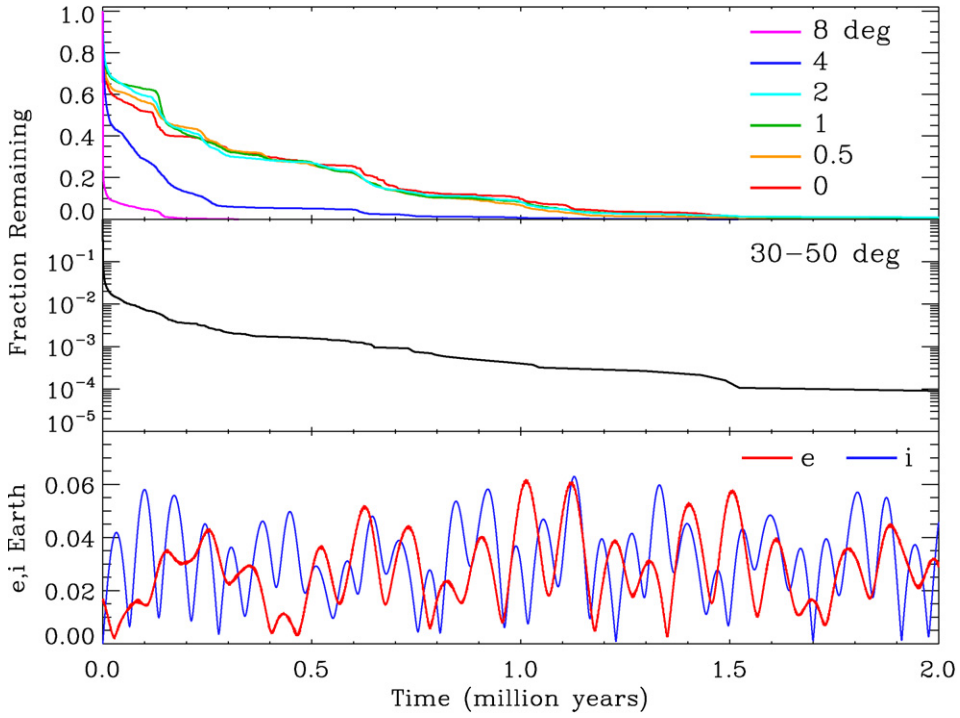

Fig. 6. The colored curves in the top panel show the fraction of particles remaining as a function of time for the run with the smallest grid (longest lifetime region) near the L_4 point (the same runs as presented in Figs. 1d and 3c) for each value of $i \leqslant 8°$ studied. The curve in the middle panel shows the fraction of particles remaining as a function of time for the runs $i \geqslant 30°$ near the L_4 point (the run presented in Fig. 5), displayed on a logarithmic scale because of the rapid early depletion. The red and blue curves in the bottom panel show, respectively, the eccentricity and sine of the inclination of Earth's orbit about the Sun on the same time scale. The correlation between these plots shows the effects of changes in Earth's heliocentric orbit on particle survival. Note that particles are lost more rapidly when the Earth's orbital eccentricity is increasing towards a high value.

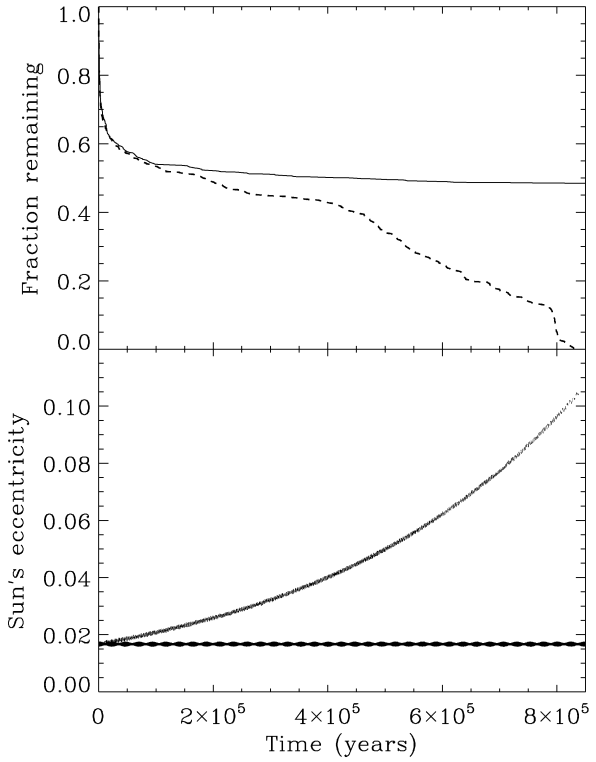

Fig. 7. Results of the integrations comparing particle survival lifetimes in the restricted 4-body problem with and without artificial increases in the eccentricity of the Earth–Sun orbit. The dashed curves in each plot show the run with e artificially excited, while the solid curves are without this acceleration.

those used in the highest resolution planar grid for the main integrations about the L_4 point (see line 4 in Table 1 and Fig. 1d). In one of the two runs, the eccentricity of the Sun was changed by applying a small acceleration at each step of the form $d\mathbf{v}/dt = 2(\mathbf{r}\cdot\mathbf{v})/(r^2\tau)\mathbf{r}$, where $\mathbf{r}\cdot\mathbf{v}$ is the dot product of the radius and velocity vectors, with τ set equal to 10^6 years. All of the particles in this run were lost within 830,000 years, whereas almost half of the particles in the integration without artificial acceleration were still in the vicinity of the L_4 point at that time (Fig. 7). This suggests that (planet-induced, in the physical problem) variations in the eccentricity of the Earth–Sun orbit, rather than any particular value of this eccentricity or direct planetary perturbations, are responsible for destabilizing the Earth–Moon triangular Lagrangian points.

3. Conclusions

The results of our eight planet numerical integrations presented above provide extremely strong evidence that all but possibly a trivially small fraction of orbits near the Earth–Moon triangular Lagrangian points are unstable on geologically short timescales.[1] Thus, it is not surprising that no natural satellites have been detected in these regions; indeed, if any small, undetected debris is in these dynamical regions, it almost certainly was placed there within the geologically recent past by non-gravitational processes such as collisions, cometary outgassing, the Yarkovsky effect or other electromagnetic forces. Moreover, our results imply that the lack of objects observed at the Earth–Moon Lagrangian points cannot be used to constrain the origin or very long term evolution of the Solar System.

Acknowledgments

This work was supported by NASA's Planetary Geology & Geophysics Program through RTOP 344-30-50-01. We thank A. Dobrovolskis for useful discussions and Matija Ćuk and an anonymous reviewer for constructive comments on the manuscript.

References

Chambers, J.E., 1999. A hybrid symplectic integrator that permits close encounters between massive bodies. Mon. Not. R. Astron. Soc. 304, 793–799.

Chambers, J.E., Quintana, E.V., Duncan, M.J., Lissauer, J.J., 2002. Symplectic integrator algorithms for modeling planetary accretion in binary star systems. Astron. J. 123, 2884–2894.

Ćuk, M., 2007. Excitation of lunar eccentricity by planetary resonances. Science 318, 244.

Ćuk, M., Gladman, B.J., Gallant, J., 2006. Lunar trojans as the source of the lunar cataclysm. In: AAS/Division for Planetary Sciences Meeting Abstracts. Abstract 66.02.

Danby, J.M.A., 1988. Fundamentals of Celestial Mechanics, second ed. Willmann–Bell, Richmond, VA.

Everhart, E., 1985. An efficient integrator that uses Gauss–Radau spacings. In: Carusi, A., Valsecchi, G.B. (Eds.), Dynamics of Comets: Their Origin and Evolution. In: ASSL, vol. 115. Kluwer, Dordrecht, pp. 185–202.

Innanen, K.A., Mikkola, S., 1989. Studies on Solar System dynamics. I. The stability of saturnian trojans. Astron. J. 97, 900–908.

Jorba, À., 2000. A numerical study on the existence of stable motions near the triangular points of the real Earth–Moon system. A dynamical systems approach to the existence of trojan motions. Astron. Astrophys. 364, 327–338.

Kokubo, E., Ida, S., Makino, J., 2000. Evolution of a circumterrestrial disk and formation of a single moon. Icarus 148, 419–436.

Lagrange, J.L., 1772. Essai sur le Problème des Trois Corps. Paris Academy, Paris.

Nesvorný, D., Dones, L., 2002. How long-lived are the hypothetical trojan populations of Saturn, Uranus, and Neptune? Icarus 160, 271–288.

Sheppard, S.S., Trujillo, C.A., 2006. A thick cloud of Neptune trojans and their colors. Science 313, 511–514.

Valdes, F., Freitas, R.A., 1983. A search for objects near the Earth–Moon Lagrangian points. Icarus 53, 453–457.

[1] A rigorous proof that no orbits are stable over the age of the Solar System would need to be done analytically. Such a proof would only apply to the "toy problem" of the motion within a Newtonian (or general relativistic) potential of the Moon–Sun–planets, because of uncertainties in processes such as the rate of lunar tidal recession, which is a very important consideration on billion year timescales.